Irreversible magnetization effects in a network of resistively shunted tunnel junctions

A. Majhofer,* T. Wolf, and W. Dieterich
Fakultät für Physik, Universität Konstanz, D-7750 Konstanz, West Germany
(Received 4 March 1991)

We investigate the magnetic behavior of a two-dimensional network of resistively-shunted (zero-capacitance) Josephson junctions, treating magnetic screening effects in a self-consistent manner. By this, we obtain stationary distributions of magnetic flux and hysteresis effects typical of single crystals or ceramic samples of high-T_c superconductors, depending upon the magnitude of the magnetic penetration depth λ_J.

I. INTRODUCTION

One of the characteristic properties of high-T_c superconductors is the strong irreversibility in their magnetic behavior. This irreversibility manifests itself, e.g., as a difference in magnetic moments of zero-field-cooled and a field-cooled sample and was found in single crystals as well as in ceramic samples.

To explain this phenomenon Müller, Takashige, and Bednorz[1] proposed the so-called "superconducting glass" model where a ceramic sample is described as a positionally disordered system of grains coupled via Josephson weak links. Extensive Monte Carlo simulations, indeed, reproduced many qualitative features of the experimental data.[2,3] Further it was argued[4] that, owing to a very short coherence length in the high-T_c crystals, twinning planes and other defects act like intrinsic weak links and lead to "glassy" behavior of magnetic domains, similar to the case of ceramics but on a much shorter length scale.

On the other hand, following the observation of an Abrikosov lattice of vortices in $YBa_2Cu_3O_7$ samples,[5] Yeshurun and Malozemoff[6] came to the conclusion that irreversible effects in high-T_c superconductors are due to a flux creep phenomenon taking place with exceptionally low activation energies. Recently, numerical simulations within a flux creep model allowing for some distribution of activation energies reproduced the time dependence of magnetic relaxation and the current-voltage characteristics of high-T_c superconductors.[7,8]

In many respects the models referred to above are complementary, since, as pointed out by Tinkham and Lobb[9] (see also Ref. 10), they focus on opposite limiting cases of the physics of strongly inhomogeneous type-II superconductors. In the superconducting glass model the role of disorder and frustration is stressed while screening effects due to the magnetic field of the Josephson currents are usually neglected.[2,3] In the flux creep model, however, the sample is treated as a type-II superconductor, and inhomogeneity is only accounted for through the pinnig energies. In this work we show that both of these views of inhomogeneous superconductors are combined within a granular model taking screening effects into account. Specifically, as a model for a finite superconducting sample subjected to an external magnetic field, we consider a system of grains placed at the sites of a two-dimensional square lattice oriented perpendicular to the external field; see Fig. 1. Each grain is characterized by a superconducting order parameter, whose magnitude is a constant for all grains, and neighboring grains are coupled via Josephson junctions. We demonstrate that a self-consistent treatment of the order parameter phases, the local magnetic flux, and the induced screening currents yields a wide spectrum of magnetic properties, ranging from a vortex lattice to spatial magnetic patterns similar to the Bean[11] model. By this we are able to reproduce the essential features of magnetic measurements reported for single crystals as well as for ceramic superconductors.

II. MODEL

As our model we consider a square lattice of Josephson junctions, displayed in Fig. 1. Generally, each junction may be characterized by its critical superconducting current I_0, its normal resistivity R, and its capacitance C. Since we are interested only in slow relaxation processes, we neglect the capacitance and use overdamped dynamics. To establish the corresponding equations of motion of our network, let us introduce the "horizontal" and "vertical" gauge-invariant phase differences θ_{ij} and ϑ_{ij}, respectively. In the absence of external currents, the current through a particular link is given by a superposition of elementary circular currents I_{ij}, see Fig. 1,

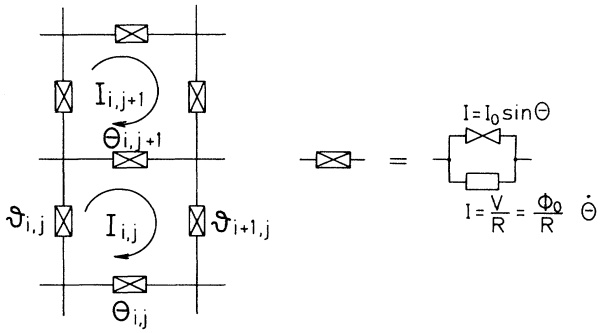

FIG. 1. A schematic view of a network of weak links used as a model of an inhomogeneous superconducting medium.

$$I_{i,j}-I_{i,j+1}=I_0\sin\theta_{i,j+1}+\frac{\phi_0}{R}\frac{d\theta_{i,j+1}}{dt}\ , \tag{1}$$

$$I_{ij}-I_{i-1,j}=I_0\sin\vartheta_{ij}+\frac{\phi_0}{R}\frac{d\vartheta_{ij}}{dt}\ , \tag{2}$$

with

$$\theta_{ij}=\Delta\varphi_{ij}-\frac{1}{\phi_0}\int \mathbf{A}\cdot d\mathbf{l}\ , \tag{3}$$

and a similar expression for ϑ_{ij}. Here, $\Delta\varphi_{ij}$ is the difference in phases of the superconducting order parameters in neighboring grains, $\phi_0=h/4\pi e$, $\mathbf{A}$ is the vector potential, and the integral is taken across the link. In this paper we are interested in the properties of the zero-field-cooled samples at temperatures well below the transition temperature for the bulk superconductor (i.e., single grain). From Eq. (3) it then follows that the magnetic flux ϕ_{ij} through a single mesh is given by[12]

$$\frac{\phi_{ij}}{\phi_0}=\vartheta_{ij}+\theta_{i,j+1}-\vartheta_{i+1,j}-\theta_{ij}\ . \tag{4}$$

On the other hand, ϕ_{ij} depends linearly on $\phi_{\rm ext}$ and all currents I_{kl}, i.e.,

$$\phi_{ij}=\phi_{\rm ext}-\sum_{kl}L_{ij,kl}I_{kl}\ . \tag{5}$$

As an approximation we only retain the self-inductance L of each lattice mesh,

$$\phi_{ij}=\phi_{\rm ext}-LI_{ij}\ . \tag{6}$$

In describing bulk materials, the neglect of mutual inductances $L_{ij,kl}$, $(ij)\neq(kl)$, would correspond to a system which is uniform along the direction of the magnetic field. Under more realistic conditions of a finite sample we expect that the approximation (6) involving a phenomenological parameter L still remains physically correct. This is supported by explicit calculations presented in the Appendix, where we discuss the effect of nearest-neighbor and next-nearest-neighbor mutual inductances.

Elimination of I_{ij} from Eqs. (1)–(4) and (6) leads to a system of ordinary differential equations for θ_{ij} and ϑ_{ij}. In the present work we only consider ordered lattices, where all links are identical. Then we obtain

$$\frac{d\vartheta_{ij}}{dt}=\frac{R}{L}(\vartheta_{i-1,j}-2\vartheta_{ij}+\vartheta_{i+1,j}+\theta_{ij}-\theta_{i-1,j}+\theta_{i-1,j+1}-\theta_{i,j+1}-\beta\sin\vartheta_{ij})\ , \tag{7}$$

$$\frac{d\theta_{ij}}{dt}=\frac{R}{L}(\theta_{i,j+1}-2\theta_{ij}+\theta_{i,j-1}+\vartheta_{ij}-\vartheta_{i,j-1}+\vartheta_{i+1,j-1}-\vartheta_{i+1,j}-\beta\sin\theta_{ij})\ . \tag{8}$$

Here we have introduced the dimensionless parameter $\beta=LI_0/\phi_0$ which determines the maximum flux difference in neighboring lattice loops, as seen from Eq (5). At the left ($i=1$) and lower ($j=1$) edge of the lattice we have the boundary conditions:

$$\frac{d\vartheta_{1j}}{dt}=\frac{R}{L}\left[\frac{\phi_{\rm ext}}{\phi_0}-\vartheta_{1j}+\vartheta_{2j}-\theta_{1,j+1}+\theta_{1j}-\beta\sin\vartheta_{1j}\right]\ , \tag{9}$$

$$\frac{d\theta_{i1}}{dt}=\frac{R}{L}\left[-\frac{\phi_{\rm ext}}{\phi_0}+\vartheta_{i1}-\vartheta_{i+1,1}+\theta_{i2}-\theta_{i1}-\beta\sin\theta_{i1}\right]. \tag{10}$$

These are obtained from Eqs. (1)–(4) and (6) by putting $I_{ij}=0$ outside the system. Analogous conditions hold for the other two boundaries. Let us remark that these conditions can be regarded as the lattice equivalent of the boundary conditions at surfaces usually assumed in the electrodynamics of continuous media. Equations (7)–(10) describe the long-time relaxation phenomena in our network. All stationary solutions depend only on the value of β and, via the boundary conditions, on the external magnetic flux $\phi_{\rm ext}$.

III. RESULTS AND DISCUSSION

We solve Eqs. (7)–(10) numerically for different $\phi_{\rm ext}$ with $\theta_{ij}=\vartheta_{ij}=0$ initially ($t=0$) and obtain the distribution of magnetic flux from Eq. (4). For an $N\times N$ network with $N=30$, which we consider here, all solutions usually reach their stationary values after times $t<500$ in units of L/R.

It is important to note that there are two characteristic length scales in the problem: the lattice constant (or grain size) a, and the magnetic penetration depth $\lambda_J=a/\sqrt{\beta}$. An estimate of the self-inductance L of one lattice mesh shows that our definition of λ_J essentially agrees with Refs. 9 and 10.

For $\beta\ll 1$ (i.e., for large λ_J) our system behaves similarly to type-II superconductors.[9,10] In small magnetic fields flux does not enter the sample and the values of ϕ_{ij} fall exponentially with distance from the boundary, with the characteristic decay length λ_J. In stronger fields flux penetrates into the system and forms there a regular lattice. Penetration of magnetic flux into the sample causes some energy to be dissipated and the whole process is irreversible. Thus, if after some time the external field is switched off, some flux remains trapped in the system. Figure 2 shows the distribution of the remanent flux corresponding to $\beta=0.1$ and initial external flux $\phi_{\rm ext}=\phi_0$. Much of the structure of a flux lattice consisting of well separated vortices is still present as a result of the mutual vortex repulsion and the local pinning barriers due to the discreteness of the system. The overall cross-like form seen in Fig. 2 is due to the system symmetry. Note that

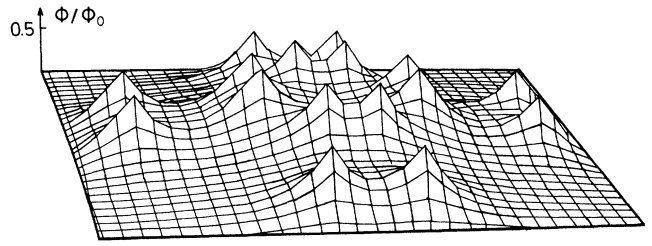

FIG. 2. Remanent magnetic flux distribution in a system of 30×30 weak links with $\beta=0.1$ and initial external flux $\phi_{ext}=\phi_0=h/4\pi e$.

near the corners the flux is expelled more easily.

The higher β, the more each lattice mesh acts like a pinning center. For $\beta>1$, when λ_J is smaller than the grain size, the picture differs qualitatively from the previous case. Each lattice mesh can accommodate several flux quanta. In particular, in the limiting case of very large β (practically for $\beta>10$) and strong magnetic fields, we find that the magnetic flux density falls linearly with distance from the boundary, with the maximum possible slope β/a. In that respect our system behaves like a hard superconductor as described within the critical state model by Bean.[11] At intermediate values of β the situation becomes more complex. As an example, in Fig. 3(a) we whow results for $\beta=2$ and $\phi_{ext}=10\ \phi_0$. The additional structure which distorts the approximately linear decrease of magnetization towards the interior of the sample results from an interplay between the effect of the external flux entering via the boundary conditions and the nonlinear restoring forces in the system, a situation similar as in the Frenkel-Kontorova model[13] subjected to external forces. Note also that for intermediate values of β the average gradient of magnetization is considerably smaller than β/a.

The effect of β on the remanent magnetization may be seen by comparing Fig. 2 with Fig. 3(b) where the remanent flux is displayed for $\beta=2$ and $\phi_{ext}=10\ \phi_0$. The escape of flux after switching off the magnetic field now creates a characteristic distribution with a maximum near the middle of the zone penetrated before [see Fig. 3(a)] and with roughly equal slopes towards the interior and the exterior of the sample. Let us remark that the overall flux distribution patterns shown in Figs. 3(a) and 3(b) are qualitatively similar to those observed in $YBa_2Cu_3O_7$ single crystals and ceramics by the high-resolution Faraday effect.[14,15]

Experimentally it is more common to measure the total magnetic moment and to investigate irreversible effects via the magnetic hysteresis. The computed magnetic hysteresis curves for $\beta=0.1$ and $\beta=2$ are shown in Figs. 4(a) and 4(b), respectively. There the quantity ϕ represents the average of ϕ_{ij} over the whole lattice. The curves were

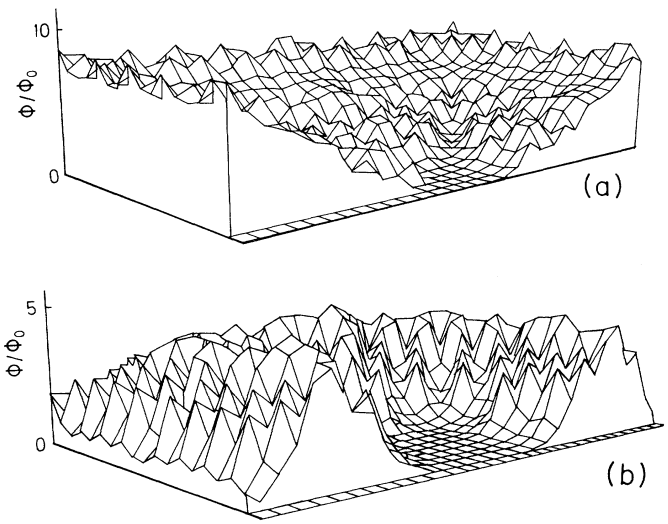

FIG. 3. (a) Magnetic flux distribution in a section of our network with $\beta=2$ after applying an external field $\phi_{ext}=10\ \phi_0$. (b) Remanent flux for an initial distribution shown in (a) after switching off the external field.

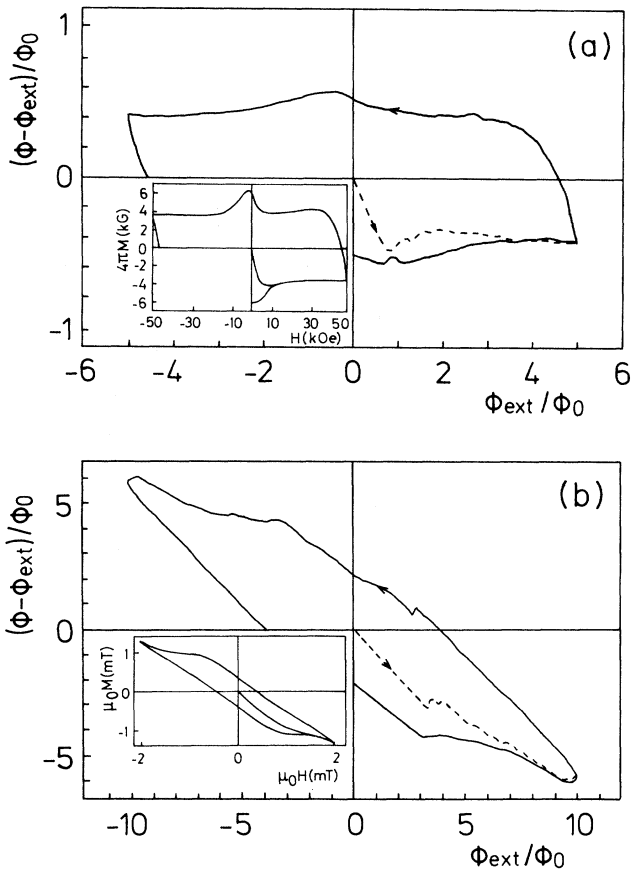

FIG. 4. Magnetic hysteresis for (a) $\beta=0.1$ and (b) $\beta=2$. The insets in (a) and (b) show experimental results for $YBa_2Cu_3O_7$ single crystals (after Ref. 16) and granular $YBa_2Cu_3O_7$ (after Ref. 18), respectively.

obtained under quasistationary conditions with changes of the external field by the order of $\frac{1}{500}$ of its maximum value after each time step. According to the previous discussion, for $\beta=0.1$ our system behaves like a homogeneous type-II superconductor, and indeed, the corresponding curve in Fig. 4(a) is qualitatively very close to the experimental results for $YBa_2Cu_3O_7$ single crystals in fields parallel to the c axis. Data by Swartzendruber *et al.*[16] are shown in the inset for comparison. In sintered $YBa_2Cu_3O_7$ samples, irreversible effects observed in very small magnetic fields are dominated by the behavior of superconducting currents through the intergrain Josephson junctions while the grains remain in the Meissner phase. The shapes of measured hysteresis curves[17,18] are very similar to our results for $\beta=2$. An illustrative example is shown in Fig. 4(b), together with measurements by Male[18] *et al.* The choice $\beta=2$ is quite representative since the corresponding values for ceramic samples vary between 0.5 and 30 (estimated from the data in Refs. 18 and 19).

In our analysis we considered here only a regular network of identical weak links and disregarded possible irregularities in the coupling constants and positions of the superconducting grains. These effects may be introduced as distributions of values of β and $\phi_{\rm ext}$ respectively. Weak links with large β act like strong pinning centers, while variations in $\phi_{\rm ext}$ are equivalent to the type of disorder considered in the superconducting glass model. These extensions are now the subject for further investigation.

In summary, we investigate here a network of weak links as a model of inhomogeneous superconductors. The magnetic flux due to the induced currents is taken into account via a self-inductance coefficient. By this we are able to qualitatively reproduce a broad spectrum of irreversible effects observed in high-T_c superconductors. Our model and its generalizations discussed above are expected to provide a consistent basis to analyze the main physical effects usually considered in the phenomenology of high-T_c superconductors, in particular phenomena that are "between" the scope of alternative models: the superconducting glass model and the giant-flux creep model.

ACKNOWLEDGMENTS

We are grateful to P. Brüll, R. Griessen, P. Leiderer, R. Schilling, and P. Ziemann for many helpful discussions. This work was supported in part by the Deutsche Forschungsgemeinschaft, SFB 306.

APPENDIX

To evaluate the effect of mutual inductances, we adopt here the approximation where $L_{ij,ij}=L, L_{ij,kl}=L_N$ for nearest-neighbor plaquettes, $L_{ij,kl}=L_{NN}$ for next-nearest-neighbor plaquettes, and $L_{ij,kl}=0$ otherwise. Then (5) takes the form

$$\phi_{ij}=\phi_{\rm ext}-LI_{ij}-L_N(I_{i-1,j}+I_{i+1,j}+I_{i,j+1}+I_{i,j-1}) -L_{NN}(I_{i-1,j-1}+I_{i-1,j+1}+I_{i+1,j-1}+I_{i+1,j+1}) . \tag{A1}$$

In the case of $\beta\ll 1$ the circular currents I_{ij} vary on length scales $\lambda_J\gg a$. Neglecting terms of order $(a/\lambda_J)^2$, the parentheses in (A1) can be replaced by $4I_{ij}$. This yields

$$\phi_{ij}=\phi_{\rm ext}-\bar{L}I_{ij} , \tag{A2}$$

with the effective inductance

$$\bar{L}=L+4(L_N+L_{NN}) . \tag{A3}$$

In the opposite limit $\beta\gg 1$ our argument relies on the linear magnetization profiles observed in Sec. III, which correspond to a linear variation of I_{ij} with distance from the surface. By this parentheses in (A1) can again be replaced by $4I_{ij}$ showing that (A2) is consistent also for $\beta\gg 1$.

Next we perform a quantitative comparison of the two approximations (A1) and (A2) for arbitrary β. The extended problem defined by (A1) is solved numerically, using representative values $L_N=-L/20$ and $L_{NN}=0.8L_N$. There is excellent agreement of the total magnetization with that obtained from the local approximation (A2) and (A3) in the cases $\beta=0.1$ and 10. For $\beta=2$ both results agree within 5%.

*Present address: Institut of Experimental Physics, Warsaw University, PL-00 681 Warsaw, ul. Hoza 69.

[1] K. A Müller, M. Takashige, and J. G. Bednorz, Phys. Rev. Lett. **58**, 1143 (1987).

[2] I. Morgenstern, K. A. Müller, and J. G. Bednorz, Z. Phys. B **69**, 33 (1987).

[3] A. Majhofer, L. Mankiewicz, and J. Skalski, Phys. Rev. B **39**, 4332 (1989); **42**, 1022 (1990).

[4] G. Deutscher and K. A. Müller, Phys. Rev. Lett. **59**, 1745 (1987).

[5] P. L. Gammel, D. J. Bishop, G. J. Dolan, J. R. Kwo, C. A. Murray, L. F. Schneemeyer, and J. V. Waszczak, Phys. Rev. Lett. **59**, 2592 (1987).

[6] Y. Yeshurun and A. P. Malozemoff, Phys. Rev. Lett. **60**, 2202 (1988).

[7] C. W. Hagen and R. Griessen, Phys. Rev. Lett. **62**, 2857 (1989).

[8] R. Griessen, Phys. Rev. Lett. **64**, 1674 (1990).

[9] M. Tinkham and C. J. Lobb, in *Solid State Physics,* edited by H. Ehrenreich and D. Turnbull (Academic, San Diego, 1989), Vol. 42.

[10] John R. Clem, Physica C **153-155**, 50 (1988).

[11] C. P. Bean, Phys. Rev. Lett. **8**, 250 (1962).

[12] A. Barone and G. Paterno, *Physics and Applications of the Josephson Effect* (Wiley, New York, 1982), Chap. 12.

[13] J. Frenkel and T. Kontorova, J. Phys. (Moscow) **1**, 137 (1939).

[14] N. Moser, M. R. Koblischka, H. Kronmüller, B. Gegenhei-

mer, and H. Theuss, Physica C **159**, 117 (1989).
[15]M. R. Koblischka, N. Moser, B. Gegenheimer, and H. Kronmüller, Physica C **166**, 36 (1990).
[16]L. J. Swartzendruber, A. Roitburd, D. L. Kaiser, F. W. Gayle, and L. H. Bennet, Phys. Rev. Lett. **64**, 483 (1990).
[17]H. Dersch and G. Blatter, Phys. Rev. **38**, 11 391 (1988).
[18]S. E. Male, J. Chilton, A. Caplin, C. N. Guy, and S. B. Newcomb, Supercond. Sci. Technol. **2**, 9 (1989).
[19]R. Marcon, R. Fastampa, and M. Giura, Phys. Rev. B **39**, 2796 (1989).